



DEVELOPMENT OF A DC TO DC BUCK CONVERTER FOR PHOTOVOLTAIC APPLICATION UTILIZING PERIPHERAL INTERFACE CONTROLLER

Z. A. Ghani¹, K. Kamit², M. Y. Zeain¹, Z. Zakaria¹, F. A. Azidin¹, N. A. A. Hadi³, A. S. M. Isira¹,
H. Othman⁴ and H. Lago⁵

¹Advanced Sensors and Embedded Control Systems (ASECs), Center for Telecommunication Research and Innovation (CeTRI), Faculty of Electronic and Computer Engineering, Universiti Teknikal Malaysia Melaka, Hang Tuah Jaya, Durian Tunggal, Melaka, Malaysia

²Department of Electrical Engineering, Politeknik Ibrahim Sultan, Masai, Johor, Malaysia

³Faculty of Electrical and Electronic Engineering Technology, Universiti Teknikal Malaysia Melaka, Hang Tuah Jaya, Durian Tunggal, Melaka, Malaysia

⁴Faculty of Engineering and Built Environment, Universiti Kebangsaan Malaysia, Bangi, Selangor, Malaysia

⁵Faculty of Engineering, Universiti Malaysia Sabah, Kota Kinabalu, Sabah, Malaysia

E-Mail: zamre@utem.edu.my

ABSTRACT

Nowadays, renewable energy has become one of the important energy resources in our daily lives. One of the important and promising renewable energy resource today is the photovoltaic (PV). However, weather changes contribute to the PV output power fluctuations. Thus, for a PV-related system, a closed-loop control system is necessary for ensuring the system produces a regulated dc output voltage. This paper presents the development of PIC16F877A microcontroller-based dc to dc buck converter. This converter steps down a dc voltage source to a specific voltage which suitable for other specific applications. For the PV output voltage fluctuating from 18V to 12V, the microcontroller generates a pulse-width modulation (PWM) signal accordingly to control the converter switching device MOSFET IRF540, thus regulating the converter output voltage to 12V. The system simulation was carried out in the PROTEUS ISIS Professional software tool. Due to the unavailability of the PV device in this simulation software, a dc voltage source is utilized. This voltage source is varied to emulate the PV output variations. The simulation results show that the controller managed to step-down the voltage source and regulated at 11.98Vdc. The prototype was built and tested in a laboratory for validation. Due to the constraints and limitations of the PV module, an adjustable power supply was used to provide variation of input voltage levels for the buck converter. The experiment results also show that the output voltage is managed to be regulated at 12V. The results signify the efficacy of developed converter control system algorithm.

Keywords: renewable energy, photovoltaic (PV), dc to dc, buck converter, pulse-width modulation (PWM), PIC16F877A microcontroller.

1. INTRODUCTION

Presently, with the advancement of technology, there is a need to look for alternative energy resources as part of the world future energy sustainability. Renewable energy resources are one of the latest technologies for the alternative energy that being used nowadays [1-2]. Some of the energy resources are sun, wind, water, etc. The world has a highly significant need for a new energy sources to replace the existing fuel. In countries where the sun shines throughout the year, solar energy is very effective and convenient to use. The use of photovoltaic (PV) modules to convert sunlight directly into electricity is very practical. PV is known as a method for generating electric power by using solar cells to convert energy from the sun into a flow of electrons.

In order to utilize the PV for delivering power to specific loads, the output needs voltage conversion. A dc to dc conversion technology is a major subject area in the field of power electronic, power engineering and drives. This conversion technique is widely adopted in industrial application and computer hardware circuits, where the simplest dc to dc conversion technology is a voltage divider, potentiometer and more. Based on the knowledge in the field of electrical engineering there are three

methods that can be used to change or reduce the value of the dc voltage to a lower dc voltage value.

Firstly, is a voltage divider; secondly are a linear voltage regulator technique and lastly a buck converter circuit [3]. The buck converter acquires the highest efficiency among other dc conversion techniques. In PV systems, power electronics circuits are utilized as a part of a PV charge controller to achieve a good productivity, accessibility and dependability. The utilization of power electronics circuits such as dc to dc converters topologies like buck converter, boost converter, buck-boost converter and other topologies as power molding hardware to supply current needed to charge battery successfully [4-7]. The converter control system in PV is capable of storing electrical energy through the battery charging process, thus, supplying energy to electrical loads such as dc motors and other home appliances.

However, the voltage produced by PV fluctuates due to the weather inconsistency and this issue needs to be addressed in the design of PV systems [8-10]. Thus, for a PV-related system, a closed-loop control system is vital for ensuring the system produces a constant dc output voltage even in the presence of PV output fluctuations [9]. In this regard, a dc to dc buck converter is integrated into



this PV system. The converter converts the output voltage generated by the PV to the desired output voltage.

The essence of the developed converter control algorithm in regulating the desired output voltage is that it specifies only a specific input voltage ranges, e.g. 18V down to 12V. Instead of using the converter output as a feedback parameter, the controller uses the input voltage as the feedback parameter. For the PV output voltage values lower than the minimum level or out of the range, no energy conversion is performed, thus conserving the system operating energy.

2. SYSTEM CONFIGURATION

The general configuration of PV system for a dc to dc buck converter is shown in Figure-1.

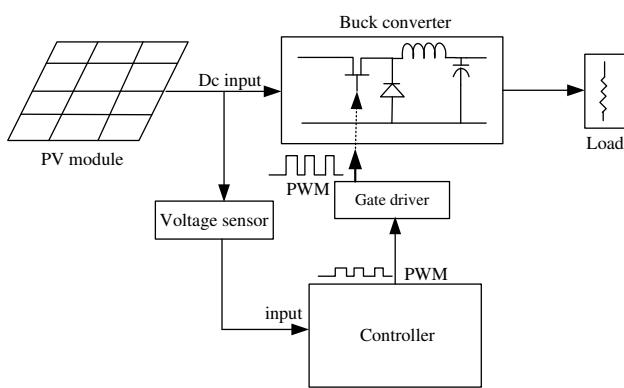


Figure-1. Configuration of PV dc to dc buck converter.

It consists of a PV module, buck converter, controller, transistor gate driver circuit, voltage sensor circuit and load. The PV module provides a dc voltage source to the buck converter which then steps it down to a specific voltage lower than the input voltage. Depending on the weather conditions, the PV exhibits the output voltage fluctuations. This voltage is measured by the voltage sensor and fed to the controller for the purpose of voltage generation and regulation.

Considering the controller input voltage level requirement which is normally 5V, the output of the voltage sensor must not exceed 5V. Based on the voltage level, the controller generates an appropriate PWM signal for the switching device such as metal oxide semiconductor field-effect transistor (MOSFET), thus generating the desired output voltage at the converter output terminal. A PWM is a switching method where the duty ratio, D of the transistor is varied [11]. A duty ratio which is represented by equation 1 is defined as the ratio of the 'on' duration, t_{on} to the switching time period, T_s [11].

$$D = \frac{t_{on}}{t_{on} + t_{off}} = \frac{t_{on}}{T_s} \quad (1)$$

It is usually expressed in the form of percentage, ranging from 0 to 98%. The transistor duty ratio is varied according to the variations of the input voltage in order to produce a constant output voltage [10-11].

Depending on the type of switching device, MOSFET for instance, a gate driver circuit is required. It converts the PWM signal voltage level to suit the device triggering level requirement

3. SYSTEM DESIGN AND SIMULATION

In this section, the design of the system and its simulation are presented.

A. SYSTEM DESIGN

The design of the buck converter system involves both hardware and software aspects.

a) Buck converter circuit design

The dc input voltage source and desired output voltage are taken into consideration in designing the buck converter circuit. The parameters are illustrated in Table-1.

Table-1. Buck converter parameters.

Parameter	Specification
Output voltage, V_{odc}	12V
Input voltage, V_i	18V ~ 12V
Load current, I_{odc}	1A
Output power, P_o	12W
Inductor current ripple, Δi_L	1.6A
Output voltage ripple, ΔV_{out}	2%
Switching frequency, f_{sw}	50 kHz.

The design of the dc to dc buck converter circuit considers the continuous current operation mode (CCM). The dc to dc buck converter is a converter that functions to step-down the dc input voltage supply to a desired dc voltage. Figure-2 shows the buck converter circuit which uses a dc input source, V_i . For this purpose, a component, Q which represents a transistor acts effectively as a switch must be used.

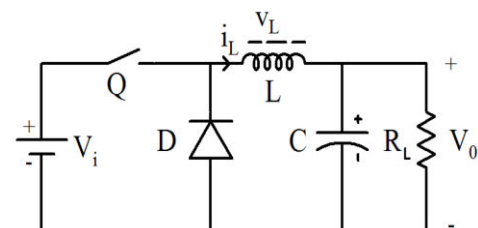


Figure-2. Buck converter with transistor in a switched off mode.

Depending on the power capacity of the circuit, semiconductor switching devices such as MOSFET, insulated-gate bipolar transistor (IGBT) and bipolar junction transistor (BJT) are suitable to carry out this task. The dc input voltage is transferred to the inductor when the transistor Q is switched on. The input current rises and flows through the inductor L and capacitor C , and load resistor, R_L and has resulted an output voltage across the



capacitor, V_o . The capacitance must be large enough so that the output voltage ripple is small.

The inductance should be of high value as to ensure the inductor current is maintained positive and in the CCM mode during the switching period. The combination of the capacitor and inductor forms a low-pass filter to reduce the output voltage fluctuations. The inductor stores energy and this energy can be used in times of need. The factors taken into account for the selection of the inductance are the peak current, current ripple, and maximum operating frequency. The detail of these selections is described in [12].

$$V_o = DV_{in} \quad (2)$$

where V_o and V_{in} are the dc output voltage and input voltage respectively.

b) Voltage sensor and gate driver

Considering the need for a stable power supply for the operation of the peripheral interface controller (PIC), a 5V voltage regulator circuit is designed as shown in Figure-3. The 220 μ F capacitors act as a stabilizer to the input and output of the regulator U1 78L05.

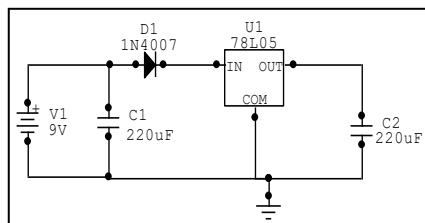


Figure-3. Voltage Regulator Circuit.

In order to measure the input voltage source, a voltage divider circuit which acts as the voltage sensor is employed. Based on the microcontroller input/output (I/O) port voltage level requirement, this circuit ensures that the input voltage must not exceeding 5V. The microcontroller generates an appropriate PWM switching signal for the MOSFET according to the input voltage level. In general, MOSFET is a voltage-controlled device and requires a gate voltage of 15V to switch on. Considering this requirement, a gate driver circuit utilizing the driver device U1 (IR2110) is designed as shown in Figure-4. This device receives a 5V level-PWM signal at pin 10 and generates a 15V level-PWM at pin 7.

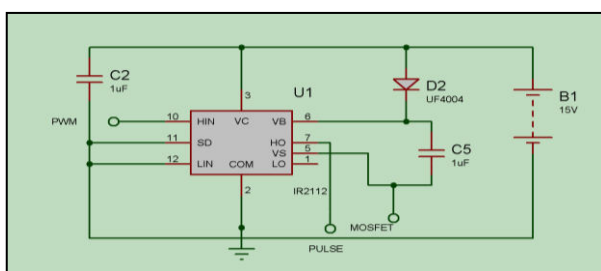


Figure-4. Gate driver circuit.

c) Software design

The PIC microcontroller is programmed in C-language and compiled using CCS compiler and then linked to the buck converter system in PROTEUS ISIS Professional. One of the most important part of the coding is the generation of the PWM signal. The following section explains the process of the PWM signal generation. The coding needs to configure the PIC I/O port pin 17 (RC2/CCP1) as an output port where the PWM signal is generated.

The generation of the PWM signal involves the I/O port module called Capture/Compare/PWM (CCP). The control register (CCP1CON) and data register (CCPR1) are often associated with the generation of PWM. The CCP1CON controls the operation of CCP1 (pin 17). This module contains a 16-bit register which can operate as a PWM Duty Cycle register. It is comprised of two 8-bit control registers which are CCPR1L (low byte) and CCPR1H (high byte). For configuring the CCP1 in PWM mode, the Timer2 type of timer resource is required.

The time base (period) and duty cycle of the PWM output need to be set. The CCP1 pin in PWM produces 10-bit resolution PWM output. The PWM period is specified by writing to the PR2 register. The period is calculated using equation 3 [13]. The frequency of the PWM is the inverse of the period.

$$T_{PWM} = [(PR2) + 1] * 4 * T_{OSC} * (TMR) \quad (3)$$

The following steps should be taken when designing the CCP1 module for PWM operation:

- Set the PWM period by writing to the PR2 register.
- Set the PWM duty cycle by writing to the CCPR1L register and CP1CON<5:4> bits.
- Make the CCP1 pin an output by clearing the appropriate TRISC<2>bit.
- Set the TMR2 prescale value, then enable Timer2 by writing to T2CON.
- Configure the CCP1 module for PWM operation.

When TMR2 is equal to PR2, the following three events occur on the next addition cycle:

- TMR2 is cleared.
- The CCP1 pin is set (exception: if PWM duty cycle=0%, the CCP1 pin will not be set).
- The PWM duty cycle is latched from CCPR1L into CCPR1H.

The PWM duty cycle is specified by writing to the CCPR1L register and to the CCP1CON<5:4> bits. The CCPR1L contains the eight most significant bits (MSBs)



And CCP1CON<5:4> bits contain the two least significant bits (LSBs). This 10-bit value is represented by CCPR1L: CCPxCON<5:4>. Equation 4 is used to calculate the PWM duty cycle in time [13]:

$$\text{PWM Duty cycle} = \frac{\text{CCPR1L: CCP1CON}\langle 5:4 \rangle}{\text{Tosc} \times (\text{TMR2Prescale Value})} \quad (4)$$

B. SYSTEM SIMULATION

For the purpose of observing the system performance and the integration of buck converter and the PIC embedded control algorithm, the simulation is conducted in PROTEUS ISIS Professional environment as shown in Figure-5.

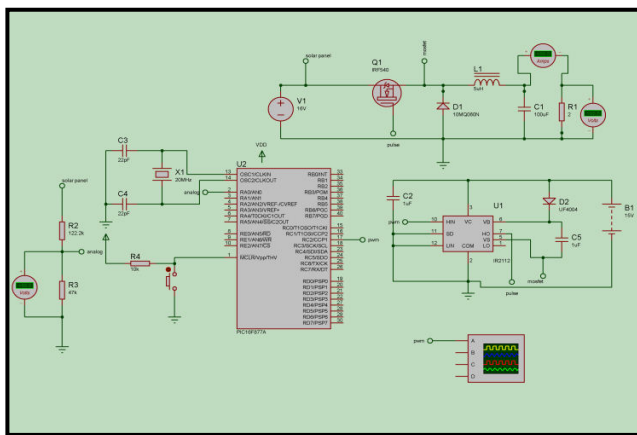


Figure-5. Simulation of buck converter in PROTEUS ISIS.

It consists of four sections which are buck converter, PIC16F877A microcontroller, voltage sensor, and gate driver. Considering the unavailability of the PV device in this simulation software, the input voltage source is set to nominal voltage of 15V. Then, this input voltage is varied to simulate the PV output voltage variations.

The microcontroller which has been loaded with the control algorithm receives and measures the dc input voltage from the voltage sensor circuit through pin 2 (RA0/AN0). Pin 2 and pin 17 (RC2/CCP1) are configured as the input and output port, respectively. By determining the level of the input voltage together with the control strategy as explained earlier, a PWM signal is generated at pin 17. For generating this switching signal, the algorithm utilizes the microcontroller PWM built-in function called Capture/Compare/PWM (CCP). The important element in the buck converter is Q1, the MOSFET model IRF540N which capable of handling high currents and high speed switching. Finally, the converter generated output voltage is connected to the resistive load.

4. EXPERIMENTAL SET-UP

Due to the constrain and limitation of the PV, an adjustable power source was used to provide variation of input voltage levels to the buck converter.

For validating the system simulation, the buck converter prototype was built and tested in a laboratory.

The in-lab experimental setups are shown in Figure-6 and Figure-7. Some of equipment used are oscilloscope, power supply and digital voltmeter panel.

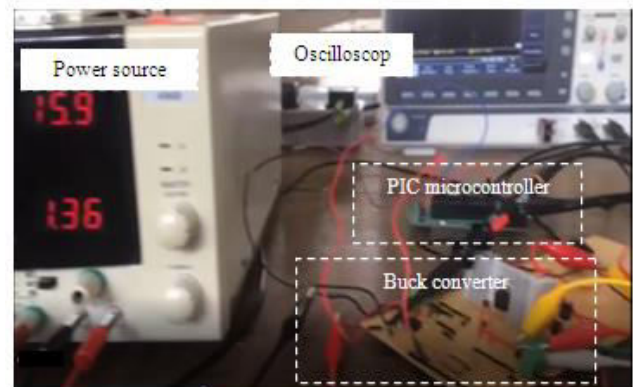


Figure-6. In-lab experimental setup showing buck converter, power source, oscilloscope and PIC microcontroller.

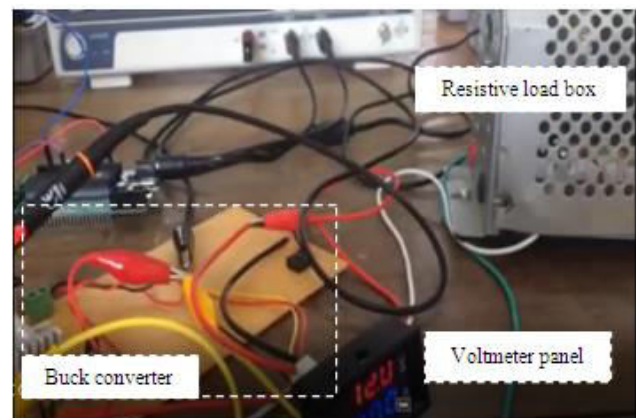


Figure-7. In-lab experimental setup showing the buck converter, resistive load box and digital voltmeter panel.

5. RESULTS AND DISCUSSIONS

In order to justify the effectiveness of the design and algorithm of the buck converter overall system operation, the simulation and experimental results are presented. In the simulation and in-lab experimental setup, the dc input voltage is varied from 17V to 12V for emulating the PV behavior and then the corresponding output responses of the system are measured.

A. Simulation results

The generated PWM switching signals for the MOSFET are depicted in Figure-8. Channel A shows the PWM waveform generated by the PIC microcontroller at pin 17 (RC2/CCP1). It is observed that, it has a peak-to-peak voltage of 5V and period of 20 microseconds. The switching frequency is calculated to be 50 kHz. The output of the gate driver is shown by Channel B.

It also has a frequency of 50 kHz and peak-to-peak voltage of 22V which suitable for triggering the MOSFET.

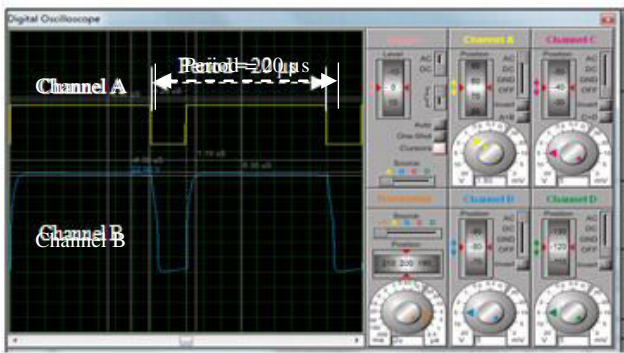


Figure-8. PWM switching waveforms observed at pin 17 of PIC and pin 7 of gate driver.

Figure-9 shows the buck converter simulation load voltage waveform for the input voltage of 15V. Initially, the waveform exhibits an overshoot at time of approximately 0.1 millisecond and gradually reaches steady state at approximately 11.98V as anticipated.

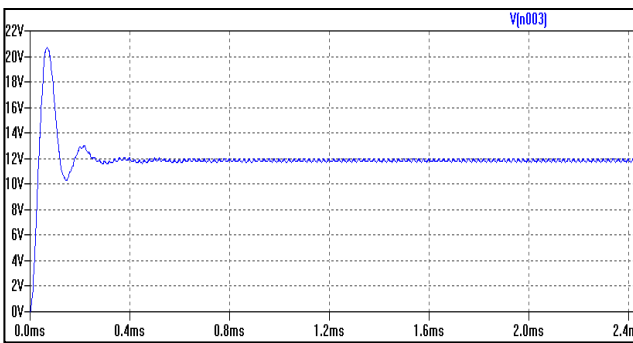


Figure-9. Simulation load voltage.

Figure-10 shows the inductor current waveform, I_L . Since the current is always positive (> 0), the buck operates in the CCM mode as expected. The triangular waveform is the result of the MOSFET switching process for a frequency of 50 kHz. As seen in the Figure, the current acquires an approximate peak of 1.75A and minimum of 0.17A. Thus, the current ripple, ΔI_L is calculated to be 1.58A as anticipated.

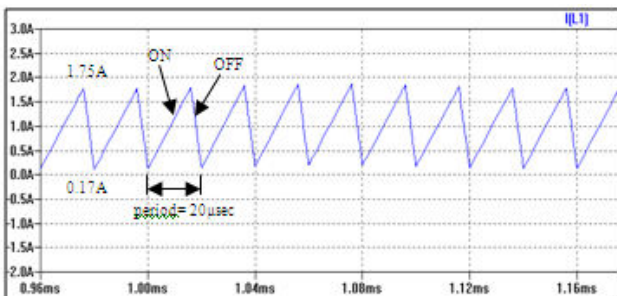


Figure-10. Current across the inductor (i_L).

Figure-11 shows the simulation load current waveform. It exhibits an overshoot at time of approximately 0.1 millisecond and gradually reaches steady state at approximately 1.05A.

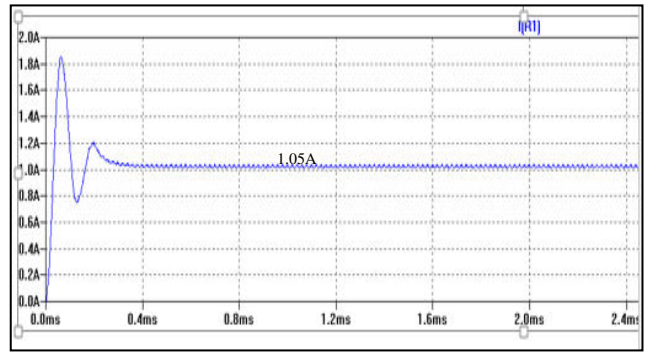


Figure-11. Output load current waveform.

The power dissipated by the load resistor is 12W as shown in Figure-12.

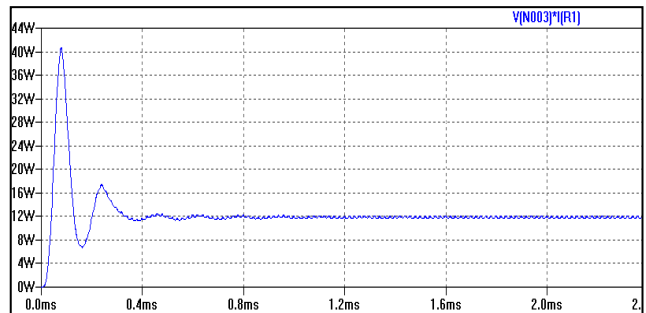


Figure-12. Power dissipated by the load.

Figure-13 shows the buck converter simulation load voltage waveform for the input voltage of 17V. Initially, the waveform exhibits an overshoot at time of approximately 0.1 millisecond and gradually reaches steady state at slightly above 12V. This shows that the system manages to regulate the output at 12.4V in spite of the changes in the input voltage.

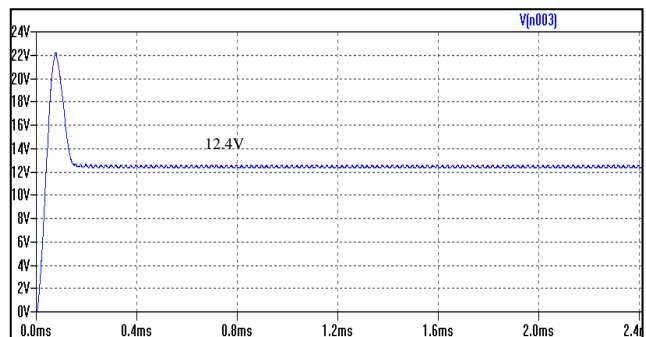


Figure-13. Load output voltage waveform.

Figure-14 shows the load output current waveform. Initially, it has a slight overshoot at approximately 0.15 milliseconds and reaches steady state at 1.07A.

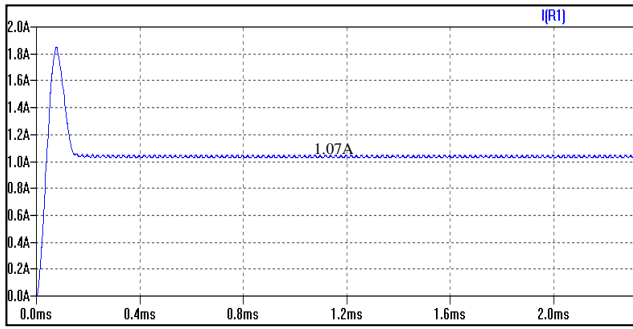


Figure-14. Output load current waveform for input voltage of 17V.

Figure-15 shows the inductor current waveform, I_L . The current shows that the system is in the CCM mode. It has the peak current of 2.2A and minimum current is closer to zero. The current ripple for the waveform, ΔI_L is 2.2A.

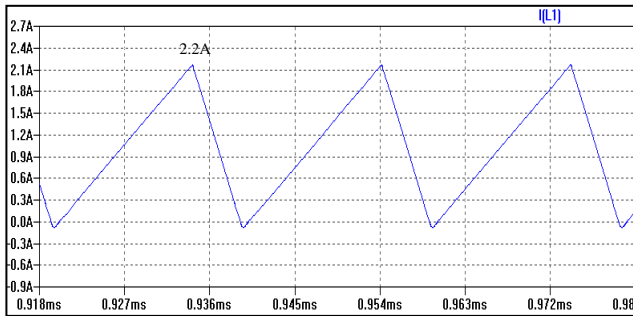


Figure-15. Inductor current waveform showing the current ripple.

Figure-16 shows the power dissipated by the load resistor, R_L which is 12.8W.

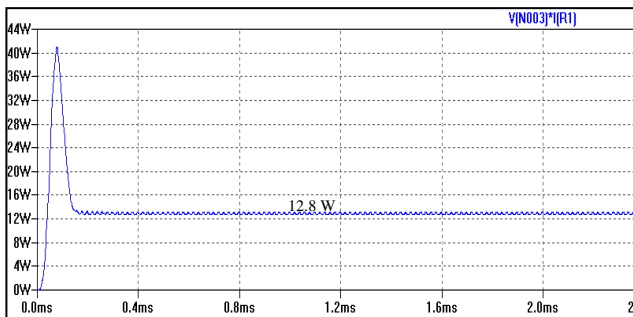


Figure-16. Power dissipated by the load resistor.

Comparisons between the design specifications and the simulation results for two different input voltages are conducted in order to observe the system performance. They are shown in Table-2 and Table-3.

Table-2. Comparison result between calculation and simulation for input voltage of 15V.

Parameter	Design	Simulation	% difference
Output voltage	12V	11.98V	0.17%
Load current	1A	1.05A	5%
Inductor ripple current	1.6A	1.56A	2.5%
Output power	12W	12.4W	3.33%

Table-3. Comparison result between calculation and simulation for input voltage of 17V.

Parameter	Design	Simulation	% difference
Output voltage	12V	12.4V	3.33%
Load current	1A	1.07A	7%
Inductor ripple current	1.6A	2.2A	37.5%
Output power	12W	12.8W	6.7%

It is observed that both design and simulation results are considered in good agreement except the inductor ripple current which shows slightly higher.

B. Experimental results

Due to some constraints in the power capacity of the PV, the experiment was carried out with the utilization of a dc power source to replace the PV.

The dc input voltage is varied manually and the parameters such as load voltage and the PWM duty cycle are recorded accordingly. Figure-17, Figure-18 and Figure-19 depict the few selected snapshots of the dc input voltage and the corresponding microcontroller PWM duty cycle. Table-4 presents the values obtained from the experiment.



Figure-17. DC input voltage showing 11.8V and corresponding PWM waveform duty cycle (99%).



Figure-18. DC input voltage showing 12.9V and corresponding PWM waveform duty cycle (91%).

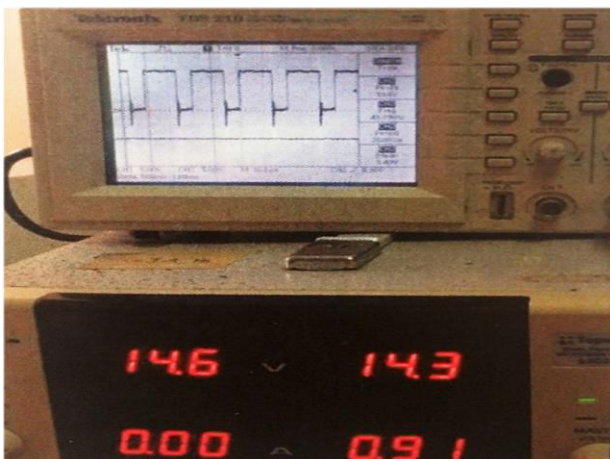


Figure-19. DC input voltage showing 14.3V and corresponding PWM waveform duty cycle (82%).

Table-4. Parameters obtained from experiment.

Input voltage (V)	Load voltage, V_{RL}	Duty cycle (%)	% voltage regulation
17.0	12.1	71	0.8
15.9	12.1	76	0.8
14.8	12.1	80	0.8
14.3	12.0	82	100
14.0	12.0	84	100
13.8	12.0	85	100
13.4	12.0	88	100
13.1	12.0	90	100
12.9	12.0	91	100
12.4	12.0	94	100
12.0	12.0	96	100
11.8	11.5	99	4.16
11.6	11.4	99	5.0

These parameters values are plotted to observe the response the buck converter dc output voltage regulation as shown in Figure-20.

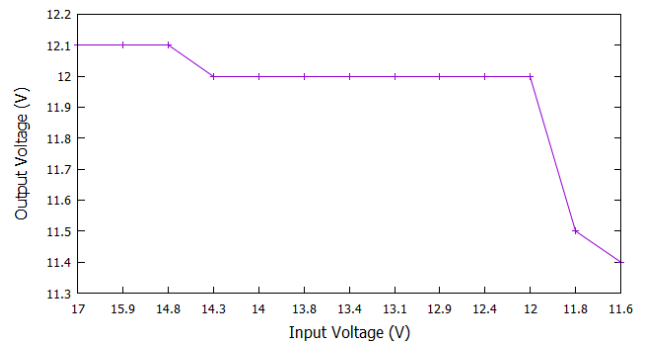


Figure-20. DC output voltage regulation.

It is observed that the output voltage is well regulated at 12V for the input voltage range of 17V to 12V. This essence of the developed buck converter control algorithm which functions to step-down the input voltage and regulated the output simultaneously. As purposely designed, any voltage level drops beyond the input voltage of 12V causes the abrupt drop of the output and gradually shut down the system as shown in the figure.

CONCLUSIONS

The development of the dc to dc buck converter for PV application utilizing the PIC16F877A microcontroller was presented in this paper. Both the converter circuit and its embedded control algorithm was developed and simulated in the PROTEUS ISIS Professional software environment. For justification, the buck converter prototype was built and tested in the laboratory. Due to the power capability constraint, the PV was replaced with a dc power supply.

Both the simulation and prototype test results showed that the developed control algorithm managed to step-down the input voltage to 12V as well as regulated it effectively. The controller managed to generate the appropriate PWM switching signal in accordance to the incoming dc input voltage. These results have shown the efficacy of the buck converter control algorithm in generating and stabilizing the desired output voltage.

REFERENCES

[1] O.C. Ruppel and B. Althusmann. 2016. Perspectives on Energy Security and Renewable Energies in Sub-Saharan Africa, Practical Opportunities and Regulatory Challenges, Second Revised and Expanded Edition.

[2] S. Romero-Hernandez and O. Romero-Hernandez. 2013. Renewable Energy in Mexico: Policy and Technologies for a Sustainable Future.



- [3] E. Fiorucci, G. Bucci, F. Ciancetta, D. Gallo, C. Landi and M. Luiso. 2013. Variable Speed Drive Characterization: Review of Measurement Techniques and Future Trends. *Advances in Power Electronics*. p. 14.
- [4] Z.A. Ghani, W.K. Wong, S. Saat, Mohd Fauzi Abd Rahman, F.A. Azidin, N.R. Mohamad. 2015. Peripheral Interface Controller-Based Photovoltaic DC-DC Boost Converter. *Journal of Telecommunication, Electronic and Computer Engineering (JTEC)*. 7(2): 13-127.
- [5] Z.M. Abdullah, O.T. Mahmood and A.M.T. Ibraheem Al-Naib. 2014. Photovoltaic battery charging system based on PIC16F877A microcontroller. *International Journal of Engineering and Advanced Technology*. 3(4): 27-31.
- [6] R.I. Putri, M. Rifa'i, M. Pujiantara, A. Priyadi, and M.H. Purnomo. 2017. Fuzzy MPPT controller for small scale stand-alone PMSG wind turbine. 2017. *ARPJ Journal of Engineering and Applied Sciences*. 12(1): 188-193.
- [7] G. Senthil Kumar and S. Indira. 2014. Embedded boost converter using voltage feedback technique. *International Journal of Research in Engineering and Technology*. 2(2): 207-212.
- [8] Z.A. Ghani, M.A. Hannan, and A. Mohamed. 2013. Simulation model linked PV inverter implementation utilizing dSPACE DS1104 controller. *Energy and Buildings*. 57: 65-73.
- [9] G. C. Sowparnika. 2015. Design and Implementation of Sliding Mode Control for Boost Converter using PV Cell. 1(10): 75-78.
- [10] P. Sathya and R. Natarajan. 2013. Design and implementation of 12V/24V closed loop boost converter for solar powered LED lighting system. *International Journal of Engineering and Technology*. 5(1): 254-264.
- [11] N. Mohan, T. Undeland and M. Robbins. 2003. *Power Electronics: Converters, Applications, and Design*. Third Edition, John Wiley & Sons, Inc., New Jersey.
- [12] M.H. Rashid. 2007. *Power Electronics Circuits, Devices and Applications*. Third Edition, Prentice-Hall of India Private Limited, New Delhi.
- [13] 2018. PIC micro Mid-range MCU family- Section 14. Compare/Capture/PWM (CCP) Module-available at: www.microchip.com/downloads/en/DeviceDoc/31014a, accessed on 31 July 2018.